HANTAVIRUS Gc GLYCOPROTEIN: EVIDENCE FOR A CLASS II FUSION PROTEIN

Nicole D. Tischler[1,2*], Angel Gonzalez[3], Tomas Perez-Acle[3], Mario Rosemblatt[1,2,4], Pablo D.T. Valenzuela[1,2,3,4]

[1]Fundación Ciencia para la Vida, [2]Instituto Milenio MIFAB, [3]Centro de Genómica y Bioinformática, Pontificia Universidad Católica and [4]Universidad Andrés Bello, Santiago, Chile.

Main text: 5502 words

Summary: 160 words

Figures: 4

Tables: 0

Supplemental Figures: 3

Supplemental Tables: 3

The GenBank accession number of the sequence reported is GI: 30313865.

*Corresponding author:

Nicole D. Tischler

Zañartu 1482

Santiago, Chile

Phone: (56 2) 239 8969

Fax: (56 2) 237 2259

E-mail address: nicole.tischler@bionova.cl

SUMMARY

Hantavirus cell entry is promoted by its envelope glycoproteins Gn and Gc through cell attachment and low pH fusion between viral and endosomal membranes. Yet the role of Gn and Gc in receptor binding and cell fusion has not been defined. In this work, a sequence presenting similar characteristics to class II fusion peptides (FP) of alphavirus E1 and flavivirus E proteins is identified within the hantavirus Gc glycoprotein. A three-dimensional comparative molecular model based on crystallographic data of tick-borne encephalitis virus (TBEV) E protein is proposed for the Andes virus (ANDV) Gc ectodomain, which supports a feasible class II fusion protein fold. *In vitro* experimental evidence is provided for the binding activity of the ANDV FP candidate to artificial membranes as demonstrated in fluorescence anisotropy assays. Taken together, our results support the hypothesis that the Gc glycoprotein of hantaviruses and of other *Bunyaviridae* members direct the viral fusion activity and may be classified as class II viral fusion protein.

INTRODUCTION

Hantaviruses belong to the family *Bunyaviridae* which encompasses five genera. Four of these include “emerging viruses”, which trigger worldwide severe diseases in humans. The best known are California encephalitis virus (*Orthobunyavirus*), Crimean-Congo hemorrhagic fever virus (*Nairovirus*), Hantaan virus (*Hantavirus*) and Sandfly fever viruses (*Phlebovirus*). *Tospovirus* is the only plant associated genus. With the exception of hantaviruses, which are transmitted by persistently infected rodents, bunyaviruses are transmitted by arthropods (Elliott, 1990).

A common feature of the *Bunyaviridae* is the presence of two glycoproteins, which are anchored in the viral envelope membrane by their C-terminal transmembrane regions. These envelope proteins are derived from a single open reading frame of the genomic ss(-) RNA medium-size segment and their size and location in the open reading frame varies between and within *Bunyaviridae* genera (Elliott, 1990). After translation, the glycoprotein precursor (GPC) is cleaved into two glycoproteins termed Gn and Gc, according to their position in the precursor. It has been suggested that these glycoproteins associate as heterodimers and accumulate in the Golgi apparatus, where viral budding takes place (Antic et al., 1992; Chen & Compans, 1991; Persson & Pettersson, 1991).

Viral glycoproteins anchored to the envelope membrane are responsible for receptor recognition and entry into target cells through fusion between viral and cellular membranes. After binding to a receptor (Gavrilovskaya et al; 1998; Kim et al., 2002), hantaviruses enter cells through clathrin dependent receptor-mediated endocytosis (Jin et al., 2002) and are thought to fuse with endosomal membranes below pH 6.3 (Arikawa et al., 1985; McCaughey et al., 1999). Although the fusogenic activity of hantavirus glycoproteins has been demonstrated, its assignment to Gn or to Gc has not been resolved (Ogino et al., 2004).

It has been proposed that the active centre of viral fusogenic proteins consists of fusion peptides (FP), which drive the initial partitioning of the fusion protein into the target membrane, and subsequently disrupt the bilayer architecture (reviewed in Epand, 2003; Nieva & Agirre, 2003).

Based on high resolution X-ray diffraction data, two fusion machineries have been recently identified (Jardetzky & Lamb, 2004). Class I encompasses fusion proteins of several unrelated viral families, among them the influenza virus haemagglutinin, the human immunodeficiency virus gp41, the paramyxovirus F and the Ebola virus GP2. Their common structural characteristics include a trimeric coiled-coil fold adjacent to the N-terminally located fusogenic unit which is composed of amino acids in alpha helical conformation (reviewed in Skehel & Wiley, 2000). In contrast, class II fusion proteins are distinguished by three domains of antiparallel beta sheet structures (Rey et al., 1995), containing an internal FP, which is formed by a loop flanked by two beta sheets (Allison et al., 2001, Levy-Mintz & Kielian, 1991). This second fusion class has been described for alphavirus E1 and flavivirus E proteins, belonging to the families *Togaviridae* and *Flaviviridae*, respectively. In spite of the differences between these fusion classes, FPs share several common physicochemical and topological parameters (reviewed in Epand, 2003; Hernandez et al., 1996; Nieva & Agirre, 2003; White et al., 1983) such as: high sequence conservation within the viral family; length of 15 to 25 residues; high Gly residue content and location in the ectodomain of envelope proteins.

Here we identify and characterize a FP candidate sequence within the Gc envelope glycoprotein of hantaviruses and of associated genera. In addition, a three-dimensional molecular model structure derived for the Gc ectodomain supports the compatibility of the hantavirus Gc glycoprotein with a class II fusion protein fold. These results suggest a role of Gc in fusion and associates hantaviruses with the class II viral fusion machinery.

METHODS

Sequence patterns and structural annotations

To achieve a complete annotation for the GPC of the human Chilean isolate CHI-7913 of the hantavirus variant Andes (ANDV) (Tischler et al., 2003; GI: 30313865), the whole sequence was scanned for transmembrane helices using the TMHMM V2.0 program (Moller et al., 2001). Secondary structures were predicted as consensus from nine different algorithms using NPS@ (Combet et al., 2000). Glycosylation sites were predicted using the PROSITE database (Gattiker et al., 2002). To identify conserved sequence regions among *Bunyaviridae* family members, the block search method was employed using the Block Maker Server (http://blocks.fhcrc.org/). Smith's MOTIF (Smith et al., 1990) and Lawrence's Gibbs sampler algorithms (Lawrence et al., 1993) were independently used for the Block search. Therefore, GPCs of the five *Bunyaviridae* genera, were extracted from the NCBI protein sequence database. Repeated sequences (100 % similarity values) were discarded. The sequence set selected for the search comprised 30 entries, six sequences per genus. In order to assure variability, the most divergent sequences in terms of identity were used. *Hantavirus* GIs: 138339, 138342, 38505526, 38505532, 442409, 30313865; *Nairovirus* GIs: 21326947, 14029592, 37730126, 401357, 59380666, 41052467; *Orthobunyavirus* Gis: 138335, 14602468, 39577664, 5823127, 30409710, 30409712; *Phlebovirus* GIs: 75198, 138341, 138345, 973315, 1174956, 52673232 and *Tospovirus* GIs: 51848026, 57157142, 18157545, 20564190, 2522489, 465409. Multiple sequence alignments were performed within each genus (6 sequences), as well as with all *Bunyaviridae* family member sequences (30 sequences) using the Blosum62 scoring matrix, as implemented in ClustalW (Higgins et al., 1994). Hidden Markov Models (HMMs) of hantavirus Gc, alphavirus E1 and flavivirus E proteins were extracted directly from the PFAM database seed groups (Bateman et al., 2004). HMM graphical representation was performed by HMM Logos (http://logos.molgen.mpg.de/), which incorporates both, emission and transition probabilities in a graphical manner (Schuster-Bockler et al., 2004).

Fold recognition methods.

The ANDV GPC sequence was divided into the glycoproteins Gn and Gc, according to the "WAASA" cleavage site (Lober et al., 2001). From the resultant Gc protein (487 aa), transmembrane and adjoining regions were excluded to reduce the false positive ratio of fold recognition programs and hence, the 414 N-terminal residues were submitted to the following fold recognition programs: 3DPSSM V2.6.0 (Kelley et al., 2000), LOOPP V3.00 (Meller & Elber, 2001) and FUGUE V2.0 (Shi et al., 2001). Outputs were ranked according to each program score values and the results were subsequently inspected for cross matches.

Comparative molecular modelling.

Hydropathicity profile comparisons were conducted through the Protein Hydrophilicity/Hydrophobicity Comparison Server (http://bioinformatics.weizmann.ac.il/hydroph/). Hydropathicity indexes were obtained according to the Kyte-Doolittle scale (Kyte & Doolittle, 1982) using a 21 residues window size and allowing gaps insertion to encourage divergent comparisons. Modeller-6 (Sali & Blundell, 1993) was used to develop several comparative models of the ANDV Gc ectodomain (residues 1 to 414), using as template the E protein crystallographic data (Rey et. al., 1995) of tick-borne encephalitis virus (TBEV) (PDBid: 1SVB). The input local alignment was manually optimized to maximize the secondary structure overlap (15.3 % identity; 24.4 % similarity). Alternatives for disulfide bridges of the model were heuristically defined by HMM comparisons of Gc and class II fusion proteins and the alignment proximity of Cys residues with the template. Twenty models were generated and ranked according to analysis of their stereochemistry using Procheck (Laskowski et al., 1993). Each model was additionally ranked by the Verify-3D score (Eisenberg et al., 1997) and potential energy values computed by Modeller. From the ensemble, the top-10 ranked structures were selected as starting structures for molecular dynamic simulations.

Molecular dynamic simulations.

Template and model structures were subjected to molecular dynamic simulations using GROMOS-96 force field (Van Gunsteren et al., 1996) within the Gromacs 3.1 software (Van der Spoel et al.,

2002). Structures were embedded in a solvent box with the simple-point charge water model to obtain a periodic boundary condition. Long-range electrostatics were calculated with the particle-mesh Ewald method. Lennard-Jones and short-range Coulombic interactions were both cut off at 0.9 nm. Simulations were performed under normal pressure and temperature conditions applying a constant pressure of 1 bar independently in all three directions with a coupling constant of p = 0.5 ps and compressibility of 4.5 e^{-5} bar^{-1}. Additionally, ions were added to compensate the net charge of the whole system. Temperature was controlled by independently coupling the protein, solvent and counterions in a 300 K temperature bath with a coupling constant of 0.1 ps. Energy minimization to reduce close contacts was achieved through the steepest-descents minimization protocol, until the maximum force decayed to 100 [kJ mol^{-1} nm^{-1}]. The system was then equilibrated to 300 K over 100 ps with 2 fs integration steps, using LINCS algorithm to restrain all bond lengths (Hess et al., 1997). After this, constraints over bonds were removed and a full 1 ns molecular dynamic simulation at 300 K was performed with 1 fs integration steps. Trajectory frames were collected each 1 ps and root mean square deviation of backbone atoms and root mean square fluctuation per residue were calculated.

Liposome preparation.

Liposomes were prepared following the method of Hope et al. (1985). Briefly, dried lipid films were hydrated with 5 mM Hepes, 150 mM NaCl, 0.1 mM EDTA (pH 7.4) and subjected to five cycles of freezing and thawing. Subsequently, vesicles were sized by extrusion through a polycarbonate filter with a pore size of 0.1 µm. Liposomes consisted of a molar ratio 1:1:1:1.5 phosphatidylcholine (from egg yolk), phosphatidylethanolamine (prepared from egg phosphatidylcholine by transphosphatidylation), sphingomyelin (from bovine brain), and cholesterol. All lipids were purchased from Avanti Polar Lipids (Alabaster, Ala, USA). The concentration of liposome suspensions was determined by phosphate analysis (Böttcher et al., 1961).

Fluorescence anisotropy of peptides.

Peptides which represent the identified conserved fusion cd-loop region residues 103-130 of the ANDV Gc sequence were synthesized in two sizes. Sequences are as follows: Gc-cd1 (residues

156 104-125) FFEKDYQYET GWGCNPGDCPGV; Gc-cd2 (residues 103-133) CFFEKDYQYE
157 TGWGCNPGDC PGVGTGCTACG. A negative control peptide derived from the ANDV Gn protein
158 (residues 80-94) VEWRKKSDTTDTTNA was also used. All fluorescence measurements were
159 performed with a Perkin-Elmer LS50 spectrofluorimeter equipped with polarizers in excitation and
160 emission beams. Temperature was maintained at 20 ºC. Small aliquots of liposomes (2.5 mM)
161 were added to a 10 μM peptide solution. The suspension was incubated for 10 min before
162 recording anisotropy through excitation at 295 nm (5 nm bandpass) and emission in L-format at
163 355 nm (10 nm bandpass). Anisotropy values were averaged from 10-15 measurements. Light
164 scattering produced by liposomes was measured by incubation of the corresponding liposome
165 concentrations with tryptophan and subtracted. The concentration of liposomes at half saturation
166 was calculated by the dissociation constant K_D of the best fitted hyperbola $r = (r_{max} \times L)/(K_D + L)$,
167 were r is the anisotropy of peptides at a given liposome concentration L and r_{max} is the anisotropy
168 of bound peptides at liposome saturation.

169

RESULTS

Detection of a FP candidate in the hantavirus Gc glycoprotein.

The sequence of the ANDV GPC was scanned in order to find properties that could relate it to either class I or class II viral fusion proteins. Figure 1a shows a complete sequence-pattern and structural annotation for the ANDV GPC, including the location of the cleavage site between the Gn and Gc glycoproteins (Lober et al., 2001), predictions for transmembrane regions, ecto- and endodomains, hydrophobic amino acid clusters, glycosylation sites and consensus secondary structures. As shown, Gn exhibits a mixture of alpha helical (21 %, red boxes) and beta strand (24 %, blue boxes) secondary structure. A higher content of residues in alpha helical conformation is present at the C-terminus, between the predicted transmembrane regions. In contrast, Gc displays predominantly a random coil (62 %) and beta strand arrangement (23 %) with a low content of alpha helices (8 %).

To identify conserved regions within hantavirus glycoproteins, the Block Database was analyzed (Henikoff & Henikoff, 1994). The most representative conserved regions over a set of 75 hantavirus sequences are shown in Figure 1a (block letters A to W). A broad conservation pattern is observed over the entire Gc sequences (block letters L to W), while a higher divergence is observed among Gn sequences (block letters A to K). Additionally, the glycoprotein sequence conservation among *Bunyaviridae* family members, including representatives of all five genera, was evaluated through sequence comparisons using the Block Maker program, scanning 30 GPC sequences with two different algorithms (Gibbs and Motif, see Methods). Five blocks were obtained which represent conserved regions among the family *Bunyaviridae*, comprising 23 of the 30 screened GPC sequences (block numbers I to V, Figure 1a). Six of the seven missing sequences belong to the genus *Phlebovirus*, thus eliminating this entire genus from further comparison analysis. The other missing GPC sequence corresponds to the more divergent Dugbe virus (GI: 401357) of the genus *Nairovirus*. Nevertheless, five of the six inspected nairovirus GPC sequences included the conserved regions. The exclusion of these sequences may be explained by the use of the stringent gap penalty employed by the block algorithms.

Since FPs are assumed to be conserved sequences within viral families, the five conserved *Bunyaviridae* blocks were analyzed for possible FP characteristics (Figure 1a). The first (I) and fourth (IV) block (ANDV GPC residues 575-594 and 606-613, respectively) were discarded as FP candidates, because of their location in the predicted endodomain of Gn. The sequences of blocks II, III and V (ANDV GPC residues 763-780, 863-877 and 766-780, respectively) fulfil the requisites of conservation, ectodomain localization, minimum length and lack of putative glycosylation sites and hence, represent suitable FP candidates.

For further studies, the sequence corresponding to blocks II and V (ANDV GPC residues 763-780) was selected based on the convergence criteria between the Gibbs and Motif block search algorithms (Figure 1a, red underlined region in Figure 1b). This region has 26.7 % identity and 86.7 % similarity within the analyzed *Bunyaviridae* sequences, showing conserved Cys, Gly and Trp residues (Figure 1b). As seen in Figure 1a, the predicted predominant secondary structure of the FP candidate region is random coiled in accordance with the high content of secondary structure breakers such as Gly and Pro residues (8 of 15 residues within ANDV). The location of this FP candidate within the first 130 residues of Gc (ANDV Gc residues 115-129), together with the predominant beta sheet secondary structure predicted for Gc, suggests that this sequence has characteristics similar to those described for class II FPs.

Hidden Markov Model (HMM) comparisons of fusion peptides.

To provide further evidence that the identified sequence shares properties with class II FPs, and to obtain position specific probabilities of the presence of key amino acids within the selected conserved region, HMMs were qualitatively compared. Figure 1c (top) shows the HMM corresponding to the hantavirus Gc region that comprises the putative FP (upper red line). The strongest position-specific probabilities belong to Trp, Cys, Gly and Pro residues. In comparison, class II FPs of flavivirus E proteins (middle) and alphavirus E1 proteins (bottom) show residues that are essential for FP functionality (see Discussion). Similarities among these three HMMs extend far beyond the putative FP region, which include highly conserved Cys residues of alphaviruses, flaviviruses (indicated by star marks) and hantaviruses (positions -12, -24 and -28, using the aromatic Trp 115 as 0 reference).

Fold recognition of the ANDV Gc protein.

To determine whether the ANDV Gc protein, which includes the putative FP, may adopt class II protein structural features, the fold of the first 414 residues of the ANDV Gc protein sequence was studied using three fold recognition programs (3DPSSM, LOOPP and FUGUE). Results obtained with 3DPSSM showed, as a first hit, the class II fusion protein E1 of Sindbis virus (PDBid: 1LD4) with an E-value of 0.03 (95 % confidence). In the case of LOOPP, the dengue 2 virus fusion protein E was obtained as a hit (PDBid: 1OK8), with a threading energy value of -164.3 (95 % of confidence). Similar results were found with FUGUE: the Semliki Forest virus fusion protein E1 (PDBid: 1RER) had a hit with a Z-score value of 2.6 (see Supplemental Tables 1-3). Hence, class II fusion proteins are the only cross-matched results. Furthermore, the majority of the threading output protein hits belong to the “mainly beta” class according to the CATH database classification.

Development and evaluation of an ANDV Gc molecular model

To further analyze if the ANDV Gc protein may support a class II fusion protein fold, a three-dimensional comparative model was derived. In order to develop such a model, the crystallographic structure of a well known class II fusion protein was used. To select such a structure, hydropathicity profiles among ANDV Gc and several class II fusion proteins with available crystallographic data were compared. These proteins included dengue virus E, TBEV E, Semliki Forest virus E1 and Sindbis virus E1. Despite the low sequence conservation among hantavirus Gc proteins and class II fusion proteins (approximately 20 %), an unexpectedly high hydropathic profile correspondence was found. The best matching profile for ANDV Gc was obtained with the E protein of TBEV (PDBid: 1SVB) (Figure 2). As expected, the Gc FP candidate and the well characterized FP of the TBEV E protein present an amphipathic nature (Figure 2), in accordance to their requirement for partition from aqueous milieu into membranes (Nieva & Agirre, 2003). Taking into account that E and E1 fusion proteins share the same topology (Lescar et al., 2001) further criteria to choose the TBEV E protein as crystallographic template were based on: (i) high quality resolution for the crystallographic structure of the TBEV E protein at 1.90Å; (ii) similar hydropathicity profiles along the complete sequences (Figure 2) and (iii) consistent overlap between the predicted and observed secondary structure elements among ANDV Gc and TBEV E

proteins (Supplemental Figure 1). Figure 3a (top) shows the best scored model of the ANDV Gc ectodomain (residues 1 to 414) in comparison with the TBEV E template crystallographic structure (bottom). As seen, the modelled structure retains a high content of beta sheet secondary structure along its three domains (Figure 3a), in accordance with the two-dimensional prediction (Figure 1a). Moreover, the FP candidate contained in the cd-loop is located in an equivalent position to the FP of TBEV E, exposing the conserved tryptophan side chain. Putative disulfide bonds involve Cys residues 87-122 and 103-129, in a manner that resembles the 1SBV structure in the FP region (Figure 3b and compare with HMMs Figure 1c). A potential third disulfide bond was assigned to the third domain between Cys residues 321-351, based on the proximity in the alignment of these residues with known disulfide pairs in the reference crystal structure (see Supplemental Figure 1).

Stereochemical and dynamic methods were used to evaluate the validity of the Gc molecular model. The stereochemical quality of the Gc model was assessed by PROCHECK, which assigned 77.4 % of the residues to the Ramachandran's plot most favoured regions, 18.9 % in additionally allowed regions, 2.5 % (nine residues) in generously allowed regions and only 1.1 % (four residues) in disallowed regions. Additional model validation using the Verify-3D program showed an overall self-compatibility score of 114, within the expected value of 188 and the lower limit of 85 accepted for a correct fold prediction. Additional evaluations to assess model stability were performed by a 1 ns full atom molecular dynamic simulation for both, the ANDV Gc 3D model and the TBEV E reference structure (see Supplemental Figure 2a and 2b).

Binding of the fusion peptide candidate to artificial membranes.

To study whether or not the putative FP identified in the Gc protein of hantaviruses has the potential to interact with membranes, experiments with synthetic peptides in the presence of artificial membranes were performed. Given that small molecules present a higher rotational movement free in solution than bound to macromolecules, the intrinsic fluorescence anisotropy of peptides was measured in their free state and in the presence of lipid vesicles. It has been shown that the fusion of flaviviruses with artificial membranes is facilitated by the presence of sphingolipids and cholesterol (Corver et al., 2000) and that these lipids are absolutely necessary

279 for alphavirus fusion (Waarts et al., 2002). For this reason, vesicles of two different compositions,
280 containing only phosphatidylcholine and containing phosphatidylcholine,
281 phosphatidylethanolamine, sphingomyelin and cholesterol, were prepared.
282 As seen in Figure 3b, the conserved FP region of class II fusion proteins (Figure 1c) encompasses
283 a loop, termed cd-fusion loop (Rey et al., 1995). To cover the cd-fusion loop (ANDV Gc residues
284 103-130), two peptides of different length were synthesized (see Methods). For fluorescence
285 experiments, the single tryptophan residue present in each peptide was employed as fluorophore.
286 Vesicle-dependent anisotropy changes as high as 0.12 for the short Gc-cd1 peptide and 0.1 for the
287 longer Gc-cd2 peptide were observed after incubation with vesicles made of phosphatidylcholine,
288 phosphatidylethanolamine, sphingomyelin and cholesterol (Figure 4). These findings show that
289 peptides free in solution decreased their rotational movement upon addition of liposomes,
290 reflecting their binding to these molecules. In comparison, no significant anisotropy changes were
291 detected when a control peptide derived from the ANDV Gn sequence was incubated with the
292 liposomes (Figure 4).
293 To further support the notion that the selected peptides interact preferably with
294 phosphatidylcholine-phosphatidylethanolamine-sphingomyelin-cholesterol membranes, their
295 affinities to the different liposome compositions were compared. When incubating the Gc-cd
296 peptides with the vesicles containing the four different lipids, the K_D value derived from each curve
297 was 15,4 μM for both Gc-cd peptides (Figure 4). When the Gc-cd1 and Gc-cd2 peptides were
298 incubated with vesicles containing only phosphatidylcholine, their K_D values were 65 μM and 96
299 μM, indicating a 4 to 6 fold lower affinity, respectively (data not shown).
300

DISCUSSION

Hantavirus fusion protein identification and classification are important steps towards the development of viral cell entry inhibitors for disease treatment. In this sense, the data presented here provide evidence for the location of an internal FP in the Gc glycoprotein of hantaviruses (Figures 1-4) and of other *Bunyaviridae* genera (Figure 1b). This peptide sequence has been described previously for its remarkable conservation within the *Bunyaviridae* (Cortez et al., 2002; Tischler et al., 2003), but its functional relevance has not been fully acknowledged. This conserved region (ANDV Gc residues 115-129) shares similar characteristics with known class II FPs of *Flaviviridae* and *Togaviridae* viruses in terms of conservation within the *Bunyaviridae* family, residue composition (aromatic, Gly and Cys residues), length (15 to 20 residues) (White et al., 1983) and secondary structure arrangement corresponding to a loop flanked by two beta sheets. Moreover, its location at approximately 100 residues from the N-terminal of the Gc protein together with the predominant beta sheet secondary structure prediction of the whole Gc protein (Figure 1a), emphasize the class II fusion protein features.

The presence of an internal FP in the hantavirus Gc protein is consistent with biochemical data from other *Bunyaviridae* members, in which the Gc protein has been associated with the viral fusion activity. Antibodies against Gc, but not against Gn of California encephalitis virus, block syncytium formation without preventing the viral attachment to the cell surface (Hacker and Hardy, 1997). In addition, an avirulent Gc variant of La Crosse virus bears a defective fusion function (Gonzalez-Sacarano et al., 1985). Furthermore, the native Gc protein presents conformational changes at the fusion pH (Pekosz & Gonzalez-Scarano, 1996), as shown for activation of other fusion proteins.

FPs traditionally have been described as hydrophobic sequences, but class II FPs also comprise charged and polar residues (see Figure 1c). They are supposed to be anchored to the target membrane by aromatic residues and are estimated to penetrate the membrane bilayer 6Å (Modis et al., 2004). The exposed carbonyls and charged residues on the outside rim of the fusion loop

are thought to impede further penetration and may interact tightly with the phospholipid heads (Gibbons et al., 2004; Modis et al., 2004). This concept coincides with the observation, that fusion of class II viruses with liposomes is a non-leaky process (Smit et al., 2002). Therefore, a hemifusion intermediate has been proposed, in which the outer leaflets of the interacting membranes have merged while the inner leaflets are still apart (Smit et al., 2002).

To provide additional arguments for a class II FP in hantaviruses, HMMs of well known flaviviruses and alphaviruses were compared with the HMM of hantaviruses (Figure 1c). It is remarkable that HMMs within the known class II FPs of alphaviruses and flaviviruses are not statistically comparable (data not shown). This might not be surprising when the low sequence conservation of approximately 20 % is considered. Therefore, their classification into class II fusion proteins is based on their unexpected structural similarity as revealed by crystallographic analysis of alphavirus E1 and flavivirus E proteins (Gibbons et al., 2004; Lescar et al., 2001; Modis et al, 2004; Rey et al., 1995). Clearly then, three-dimensional structures of proteins may be more conserved than suggested by sequence comparison.

Hence, sequences of class II FPs seem to be quite variable among different viral families, except for particular residues involved in their functionality. These residues seem to be more conserved in terms of physical-chemical properties, rather than in terms of sequence. In this sense, the identified FP candidate of hantaviruses shows a high conservation of the required aromatic and Gly residues necessary for interaction with membranes as well as Cys residues presumably involved in structure stabilization (Figure 1b and 1c). The location of conserved Cys residues in the hantavirus HMM in homologous positions to Cys residues of class II FPs far beyond the conserved FP candidate region may imply similar roles (Figure 1c). Cys residues included in class II FPs are known to stabilize by three to four disulfide bridges the fusion loop, which is located at the tip of domain II (Rey et al., 1995, Lescar et al., 2001). In summary, the similarity in sequence composition between the hantavirus FP candidate and class II FPs reinforces the hypothesis that the hantavirus Gc protein may contain a class II-like FP.

352 Evidence for the functionality of the identified FP candidate region is provided by their potential to
353 interact with artificial membranes. The intrinsic fluorescence anisotropy assays clearly
354 demonstrated the interaction of synthetic hantavirus FP candidates with lipid vesicles (Figure 4).
355 Their higher affinity to liposomes containing sphingomyelin and cholesterol coincides with
356 membrane compositions known to facilitate fusion (Corver et al., 2000) or to be required for the
357 fusion of class II viruses with liposomes (Waarts et al., 2002).

358 To study whether the hantavirus Gc protein may adopt a class II fusion protein fold, a three-
359 dimensional model was derived. Despite the low sequence similarity between hantavirus Gc and
360 class II fusion proteins (approximately 20 %), encouraging results on prediction of class II fusion
361 proteins by three different fold recognition programs (Supplemental Tables 1-3) persuaded model
362 development. Although no unique set of outputs was generated by these programs, these results
363 support strongly the notion of a beta fold structure of Gc and suggest the compatibility of the ANDV
364 Gc sequence with a class II fusion protein fold in terms of energy values and secondary structure
365 arrangement. In addition, a strong correspondence of hydropathicity profiles and secondary
366 structures between hantavirus Gc and class II fusion proteins was observed, achieving the best
367 consensus with the TBEV E protein (Figure 2 and Supplemental Figure 1).
368 The ANDV Gc model satisfies the acceptance requirements of applied stereochemical parameters
369 and structural stability by means of molecular dynamic simulations with backbone coordinate
370 deviations below 3Å in a 1 ns trajectory analysis (Supplemental Figure 2). Since in the Gc model
371 some Cys residues appear unpaired despite their close location in the 3D space, further model
372 improvements need to be focused on disulfide pair formations (Supplemental Figure 3). However,
373 trajectory analysis data indicate that the three proposed disulfide bridges seem to be the minimal
374 number that guarantees the structural stability of the proposed model. In summary, these results
375 suggest that the hantavirus Gc protein is compatible with a class II fusion protein fold and confirm
376 its possible association with this class of viral fusion machinery.

377 The association of bunyavirus Gc proteins with class II fusion proteins coincides moreover in their
378 overall arrangement. Class II fusion proteins are synthesized as polyproteins together with a N-

terminal companion glycoprotein that acts as a chaperone to avoid their aggregation (Marquardt and Helenius, 1992) and probably suppress their activation in the Golgi network (Guirakhoo et al., 1992; Mandl et al., 1991), as is the case for P62 in alphaviruses (Andersson et al., 1997) and prM in flaviviruses (Konishi et al., 1993; Lorenz et al., 2002). Such a role could also be ascribed to bunyavirus Gn proteins, since Gc does not enter the Golgi apparatus when expressed in absence of Gn (Persson & Pettersson, 1991; Shi & Elliott, 2002).

Class II fusion proteins are not merely responsible for fusion processes, as they also determine the viral envelope protein shell of icosahedral symmetry in either homodimeric or heterodimeric associations (Strauss & Strauss, 2001). Hence, the proposed similarity of *Bunyaviridae* Gc proteins with class II fusion proteins would also influence the viral morphology. In line with this notion, regularly spaced surface projections have been described for some bunyavirions (Martin et al., 1985; McCormick et al., 1982, White et al., 1982) and even an icosahedral surface organization has been proposed for these viruses (Von Bonsdorff & Pettersson, 1975; Ellis et al., 1981; Lee & Cho, 1981). Furthermore, based on the observation that the proteolytic removal of the glycoproteins produces highly deformable virion shapes, it has been hypothesized that the structural stability of bunyavirions might be conferred by the spike glycoproteins themselves (Von Bonsdorff & Pettersson, 1975). Due to the absence of a matrix protein that mediates the association and stabilization between viral envelope and nucleocapsid, a highly organized structure of the surface glycoproteins of bunyaviruses may be plausible and of clear advantage for virion stability.

In conclusion, the characteristics described here for hantavirus and other *Bunyaviridae* Gc proteins, suggest their role in cell fusion and associate them with class II fusion proteins. Furthermore, these findings raise the question whether Gn and Gc envelope glycoproteins may be involved in distinctive roles such as receptor binding, nucleocapsid interaction and fusion, as described for alphavirus E1 and E2 proteins. To confirm the participation of the proposed FP in the hantavirus fusion activity additional studies are required, including site directed mutagenesis.

405 Finally, the proposed three-dimensional Gc model can be of value in the development of cell entry
406 inhibitors that could be useful in therapy.
407

ACKNOWLEDGEMENTS

We thank Dr. Milton De la Fuente from the Universidad de Chile for the advice in preparation of liposomes and Dr. Octavio Monasterio and Dr. Esteban Nova from the Universidad de Chile for valuable anisotropic discussions and the use of their fluorescence spectrometer facilities. Our special thanks to Dr. Bernardita Méndez for a critical review of the manuscript.

REFERENCES

Allison, S.L., Schalich, J., Stiasny, K., Mandl, C.W. & Heinz, F.X. (2001). Mutational Evidence for an Internal Fusion Peptide in Flavivirus Envelope Protein E. *J Virol* **75**, 4268-4275.

Andersson, H., Barth, B.U., Ekstrom, M., & Garoff, H. (1997). Oligomerization-dependent folding of the membrane fusion protein of Semliki Forest virus. *J Virol* **71**, 9654-9663.

Antic, D., Wright, K.E. & Kang, C.Y. (1992). Maturation of Hantaan virus glycoproteins G1 and G2. *Virology* **189**, 324-328.

Arikawa, J., Takashima, I. & Hashimoto, N. (1985). Cell fusion by haemorrhagic fever with renal syndrome (HFRS) viruses and its application for titration of virus infectivity and neutralizing antibody. *Arch Virol* **86**, 303-313.

Bateman, A., Coin, L., Durbin, R. & 10 other authors (2004). The Pfam protein families database. *Nucleic Acids Res* **32** Database issue, D138-41.

Böttcher, C.J.F., Van Gent, C.M. & Pries, C. (1961). A rapid and sensitive sub-micro phosphorus determination. *Anal Chim Acta* **24**, 203-204.

Chen, S.Y. & Compans, R.W. (1991). Oligomerization, transport, and Golgi retention of Punta Toro virus glycoproteins. *J Virol* **65**, 5902-5909.

Combet, C., Blanchet, C., Geourjon, C. & Deléage, G. (2000). NPS@: network protein sequence analysis. *Trends Biochem Sci* **25**,147-150.

Cortez, I., Aires, A., Pereira, A.M., Goldbach, R., Peters, D. & Kormelink, R. (2002). Genetic organisation of Iris yellow spot virus M RNA: indications for functional homology between the G(C) glycoproteins of Tospoviruses and animal-infecting bunyaviruses. *Arch Virol* **147**, 2313-2325.

Corver, J., Ortiz, A., Allison, S.L., Schalich, J., Heinz, F.X. & Wilschut, J. (2000). Membrane fusion activity of tick-borne encephalitis virus and recombinant subviral particles in a liposomal model system. *Virology* **269**, 37-46.

Eisenberg, D., Luthy, R. & Bowie, J.U. (1997). VERIFY3D: assessment of protein models with three-dimensional profiles. *Methods Enzymol* **277**, 396-404.

Elliott, R.M. (1990). Molecular biology of the Bunyaviridae. *J Gen Virol* **71**, 501-522.

Ellis, D.S., Southee, T., Lloyd, G., Platt, G.S., Jones, N., Stamford, S., Bowen, E.T. & Simpson, D.I. (1981). Congo/Crimean haemorrhagic fever virus from Iraq 1979: I. Morphology in BHK21 cells. *Arch Virol* **70**, 189-198.

Epand, R.M. (2003). Fusion peptides and the mechanism of viral fusion. *Biochim Biophys Acta* **1614**, 116-121.

Gattiker, A., Gasteiger, E. & Bairoch, A. (2002). ScanProsite: a reference implementation of a PROSITE scanning tool. *Appl Bioinformatics* **1**, 107-108.

Gavrilovskaya, I.N., Shepley, M., Shaw, R., Ginsberg, M.H. & Mackow, E.R. (1998). Beta3 Integrins mediate the cellular entry of hantaviruses that cause respiratory failure. *Proc Natl Acad Sci U S A* **95**, 7074-7079

Gibbons, D.L., Vaney, M.C., Roussel, A., Vigouroux, A., Reilly, B., Lepault, J., Kielian, M. & Rey, F.A. (2004). Conformational change and protein–protein interactions of the fusion protein of Semliki Forest virus. *Nature* **427**, 320-325.

Gonzalez-Scarano, F., Janssen, R.S., Najjar, J.A., Pobjecky, N. & Nathanson, N. (1985). An avirulent G1 glycoprotein variant of La Crosse bunyavirus with defective fusion function. *J Virol* **54**, 757-763.

Guirakhoo, F., Bolin, R.A. & Roehrig, J.T. (1992). The Murray Valley encephalitis virus prM protein confers acid resistance to virus particles and alters the expression of epitopes within the R2 domain of E glycoprotein. *Virology* **191**, 921-31.

Hacker, J.K. & Hardy, J.L. (1997). Adsorptive endocytosis of California encephalitis virus into mosquito and mammalian cells: a role for G1. *Virology* **235**, 40-47.

Henikoff, S. & Henikoff, J. G. (1994). Protein family classification based on searching a database of blocks. *Genomics* **19**, 97-107.

Hernandez, L.D., Hoffman, L.R., Wolfsberg, T.G. & White, J.M. (1996). Virus-cell and cell-cell fusion. *Annu Rev Cell Dev Biol* **12**, 627-661.

Hess, B., Bekker, H., Berendsen, H. J. C. & Fraaije, J. G. E. M. (1997). LINCS: a linear constraint solver for molecular simulations. *J Comp Chem* **18**, 1463–1472.

Higgins, D., Thompson, J., Gibson, T. Thompson, J.D., Higgins, D.G. & Gibson, T.J. (1994). CLUSTAL W: improving the sensitivity of progressive multiple sequence alignment through sequence weighting, position-specific gap penalties and weight matrix choice. *Nucleic Acids Res* **22**, 4673-4680.

Hope, M.J., Bally, M.B., Webb, G. & Cullis, P.R. (1985). Production of large unilamellar vesicles by a rapid extrusion procedure. *Biochim Biophys Acta* **812**, 55-65.

Jardetzky, T.S. & Lamb, R.A. (2004). Virology: A Class Act. *Nature* **427**, 307-308.

Jin, M., Park, J., Lee, S & 7 other authors (2002). Hantaan virus enters cells by clathrin-dependent receptor-mediated endocytosis. *Virology* **294**, 60-69.

Kabsch, W. & Sander, C. (1983). Dictionary of protein secondary structure: pattern recognition of hydrogen-bonded and geometrical features. *Biopolymers* **22**, 2577-2637.

Karlin, S. & Altschul, S.F., (1990). Methods for assessing the statistical significance of molecular sequence features by using general scoring schemes. *Proc Natl Acad Sci USA* **87**, 2264–2268.

Kelley, L., MacCallum, R. & Sternberg, M. (2000). Enhanced Genome Annotation using Structural Profiles in the Program 3D-PSSM. *J Mol Biol* **299**, 501-522.

Kim, T.Y., Choi, Y., Cheong, H.S. & Choe, J. (2002). Identification of a cell surface 30 kDa protein as a candidate receptor for Hantaan virus. *J Gen Virol* **83**, 767-773.

Konishi, E. & Mason, P.W. (1993). Proper maturation of the Japanese encephalitis virus envelope glycoprotein requires cosynthesis with the premembrane protein. *J Virol* **67**, 1672-1675.

Kyte, J. & Doolittle, R.F. (1982). A Simple Method for Displaying the Hydropathic Character of a Protein. *J Mol Biol* **157**, 105-142.

Laskowski, R., MacArthur, M., Moss, D. & Thornton, J. (1993). PROCHECK: a program to check the stereochemical quality of protein structures. *J Appl Cryst* **26**, 283-291.

Lawrence, C.E., Altschul, S.F., Boguski, M.S., Liu, J.S., Neuwald, A.F. & Wootton, J.C. (1993). Detecting Subtle sequence signals: a Gibbs sampling strategy for multiple alignment. *Science* **262**, 208-214.

Lee, H.W. & Cho, H.J. (1981). Electron microscope appearance of Hantaan virus, the causative agent of Korean haemorrhagic fever. *Lancet* **1 (8229)**, 1070-1072.

Lescar, J., Roussel, A., Wien, M.W., Navaza, J., Fuller, S.D., Wengler, G., Wengler, G. & Rey, F.A. (2001). The Fusion Glycoprotein Shell of Semliki Forest Virus: An Icosahedral Assembly Primed for Fusogenic Activation at Endosomal pH. *Cell* **105**, 137-148.

Levy-Mintz, P. & Kielian, M. (1991). Mutagenesis of the putative fusion domain of the Semliki Forest virus spike protein. *J Virol* **65**, 4292-4300.

Lober, C., Anheier, B., Lindow, S., Klenk, H.D. & Feldmann, H. (2001). The Hantaan virus glycoprotein precursor is cleaved at the conserved pentapeptide WAASA. *Virology* **289**, 224-229.

Lorenz, I.C., Allison, S.L., Heinz, F.X. & Helenius, A. (2002). Folding and dimerization of tick-borne encephalitis virus envelope proteins prM and E in the endoplasmic reticulum. *J Virol* **76**, 5480-5491.

Mandl, C.W., Holzmann, H. & Kunz, C. (1991). Fusion activity of flaviviruses: comparison of mature and immature (prM-containing) tick-borne encephalitis virions. *J Gen Virol* **72**,1323-1329.

Marquardt, T. & Helenius, A. (1992). Misfolding and Aggregation of Newly Synthesized Proteins in the Endoplasmic Reticulum. *J Cell Biol* **117**, 505-513.

Martin, M.L., Lindsey-Regnery, H., Sasso, D.R., McCormick, J.B. & Palmer, E. (1985). Distinction between Bunyaviridae genera by surface structure and comparison with Hantaan virus using negative stain electron microscopy. *Arch Virol* **86**, 17-28.

McCormick, J.B., Sasso, D.R., Palmer, E.L. & Kiley, M.P. (1982). Morphological identification of the agent of Korean haemorrhagic fever (Hantaan virus) as a member of the Bunyaviridae. *Lancet* **1 (8275)**, 765-768.

McCaughey, C., Shi, X., Elliot, R.M., Wyatt, D.E., O'Neill, H.J. & Coyle, P.V. (1999). Low pH-induced cytopathic effect--a survey of seven hantavirus strains. *J Virol Methods* **81**, 193-197.

Meller, J. & Elber, R. (2001). Linear Optimization and a double Statistical Filter for protein threading protocols. *Proteins* **45**, 241-261.

Modis, Y., Ogata, S., Clements, D. & Harrison, S.C. (2004). Structure of the dengue virus envelope protein after membrane fusion. *Nature* **427**, 313-319.

Moller, S., Croning, M.D.R. & Apweiler, R. (2001). Evaluation of methods for the prediction of membrane spanning regions. *Bioinformatics* **17**, 646-653.

Nieva, J.L. & Agirre, A. (2003). Are fusion peptides a good model to study viral cell fusion? *Biochim Biophys Acta* **1614**, 104-115.

Ogino, M., Yoshimatsu, K., Ebihara, H., Araki, K., Lee, B.H., Okumura, M. & Arikawa, J. (2004). Cell fusion activities of Hantaan virus envelope glycoproteins. *J Virol* **78**, 10776-10782.

Pekosz, A. & Gonzalez-Scarano, F. (1996). The extracellular domain of La Crosse virus G1 forms oligomers and undergoes pH-dependent conformational changes. *Virology* **225**, 243-247.

Persson, R. & Pettersson, R.F. (1991). Formation and intracellular transport of a heterodimeric viral spike protein complex. *J Cell Biol* **112**, 257-266.

Rey, F. A., Heinz, F. X., Mandl, C., Kunz, C. & Harrison, S. C. (1995). The envelope glycoprotein from tick-borne encephalitis virus at 2 Å resolution. *Nature* **375**, 291-298.

Sali, A. & Blundell, T.L. (1993). Comparative protein modelling by satisfaction of spatial restraints. *J Mol Biol* **234**, 779-815.

Schuster-Böckler, B., Schultz, J. & Rahmann, S. (2004). HMM Logos for visualization of protein families. *BMC Bioinformatics* **5**, 7.

Shi, J., Blundell, T.L. & Mizuguchi, K. (2001). FUGUE: sequence-structure homology recognition using environment-specific substitution tables and structure-dependent gap penalties. *J Mol Biol* **310**, 243-257.

Shi, X. & Elliott, R.M. (2002). Golgi localization of Hantaan virus glycoproteins requires coexpression of G1 and G2. *Virology* **300**, 31-38.

Skehel, J.J. & Wiley, D.C. (2000). Receptor Binding and Membrane Fusion in Virus Entry: The Influenza Hemagglutinin. *Annu Rev Biochem* **69**, 531–569.

Smit, J.M., Li, G., Schoen, P., Corver, J., Bittman, R., Lin, K.C. & Wilschut, J. (2002). Fusion of alphaviruses with liposomes is a non-leaky process. *FEBS Lett* **521**, 62-66.

Smith, H.O., Annau, T.M. & Chandrasegaran, S. (1990). Finding sequence motifs in groups of functionally related proteins. *Proc Natl Acad Sci USA* **87**, 826-830.

Strauss, J.H. & Strauss, E.G. (2001). Virus Evolution: How does an enveloped virus make a regular structure? *Cell* **105**, 5-8.

Tischler, N.D., Fernandez, J., Muller, I. & 7 other authors (2003). Complete sequence of the genome of the human isolate of Andes virus CHI-7913: comparative sequence and protein structure analysis. *Biol Res* **36**, 201-210.

Van der Spoel, D., van Buuren, A. R., Apol, E. & 9 other authors (2002). *Gromacs User Manual,* version 3.1.1, Nijenborgh 4, 9747 AG Groningen, The Netherlands. Internet: www.gromacs.org.

Van Gunsteren, W. F., Billeter, S. R., Eising, A. A., Hünenberger, P. H., Kruger, P., Mark, A. E., Scott, W. R. P. & Tironi, I. G. (1996). Biomolecular Simulation: *The GROMOS96 manual and user guide*. Zürich, Switzerland: Hochschulverlag AG der ETH Zürich.

Von Bonsdorff, C.H. & Pettersson, R. (1975). Surface structure of Uukuniemi virus. *J Virol* **16**, 1296-1307.

Waarts, B.L., Bittman, R. & Wilschut, J. (2002). Sphingolipid and cholesterol dependence of alphavirus membrane fusion. Lack of correlation with lipid raft formation in target liposomes. *J Biol Chem* **277**, 38141-38147.

White, J.D., Shirey. F.G., French. G.R., Huggins. J.W., Brand, O.M. & Lee, H.W. (1982). Hantaan virus, aetiological agent of Korean haemorrhagic fever, has Bunyaviridae-like morphology. *Lancet* **1 (8275)**, 768-771.

White, J., Kielian, M. & Helenius, A. (1983). Membrane fusion proteins of enveloped animal viruses. *Q Rev Biophys* **16**, 151-195.

FIGURES

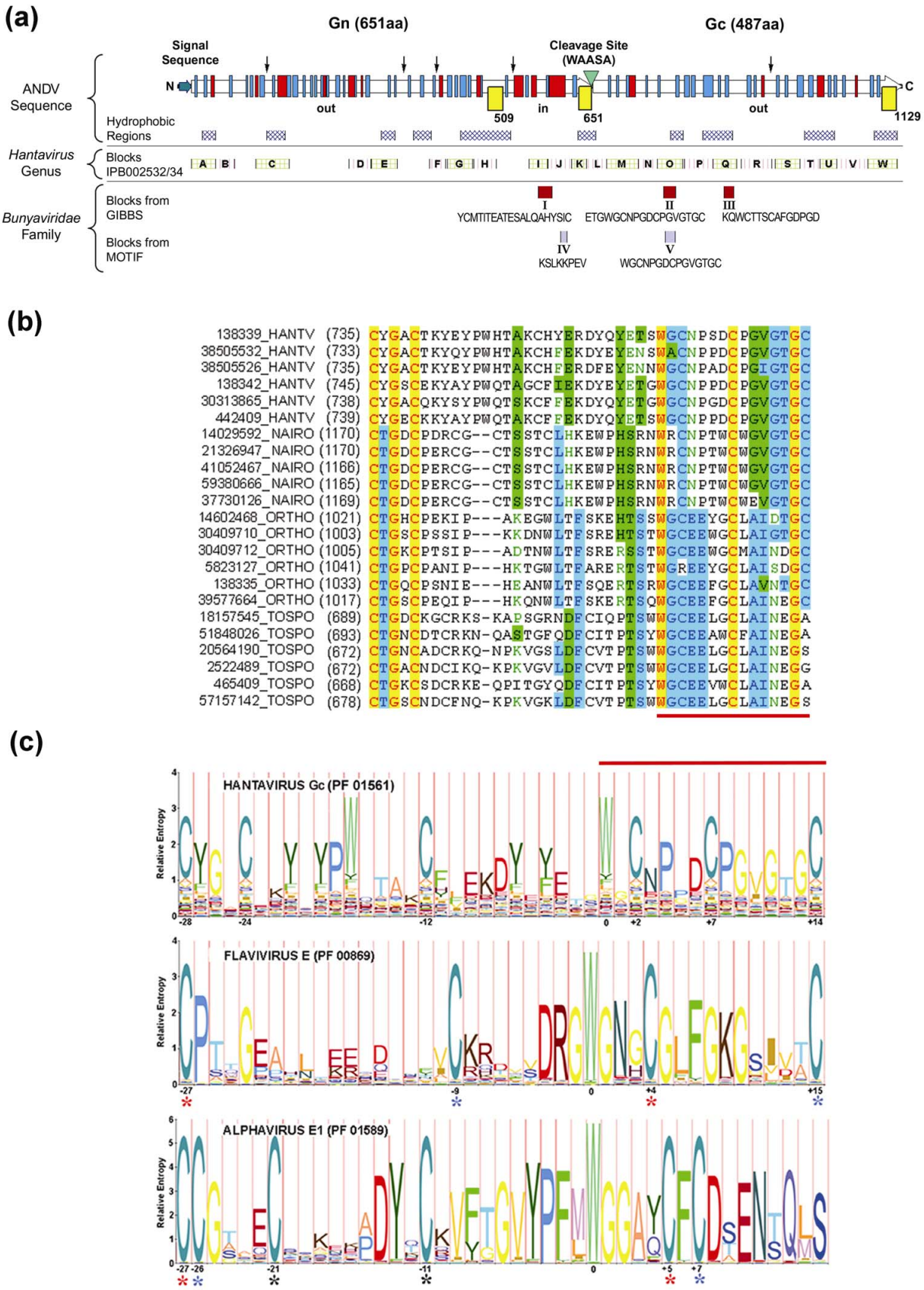

Figure 1. Structural domains and conserved regions analysis of *Bunyaviridae* glycoprotein sequences and comparison with class II fusion proteins.

a) One dimensional representation of the ANDV GPC. The WAASA cleavage site appears as green arrowhead. Secondary structure predictions appear as red boxes for alpha helices, blue boxes for beta sheets and the unboxed white regions for random coils. Predicted transmembrane regions are shown in yellow boxes with a residue number indicating the terminus. Black arrows point to predicted glycosylation sites. IN/OUT nomenclature defines the proteins endo- and ectodomains. Blue crossline filled squares represent predicted hydrophobic areas. Conserved blocks within hantaviruses appear square marked containing capital letters A to W. Conserved blocks within the *Bunyaviridae* appear in filled squares indicated by subscript Roman numbers I to V. Their corresponding sequence in the ANDV GPC sequence is indicated below.

b) Multiple sequence alignment of the FP candidates from GPC sequences of *Hantavirus*, *Orthobunyavirus*, *Nairovirus* and *Tospovirus* genera. GenBank accession numbers appear at the beginning of each sequence followed by the corresponding genus. Colours indicate as follows: identical residues in red letters and yellow background (B); conserved residues in dark blue letters and light blue B; block of similar residues in black letters and green B; weakly similar residues in green letters and white B and non-similar residues in black letters and white B. The red line at the bottom indicates the conserved region detected by the Block Maker program (*Bunyaviridae* blocks II and V).

c) HMMs of hantavirus FP candidates and class II FPs in Logos representation. PFAM accession numbers appear within parenthesis. The relative residue position number is displayed on the x-axis using the conserved Trp residue as 0 reference. Star marks indicate the Cys residues involved in disulfide bridges according to crystal structures of flavivirus E (PDBid: 1SVB) and alphavirus E1 (PDBid: 1RER). Identical colour stars indicate the disulfide pairs.

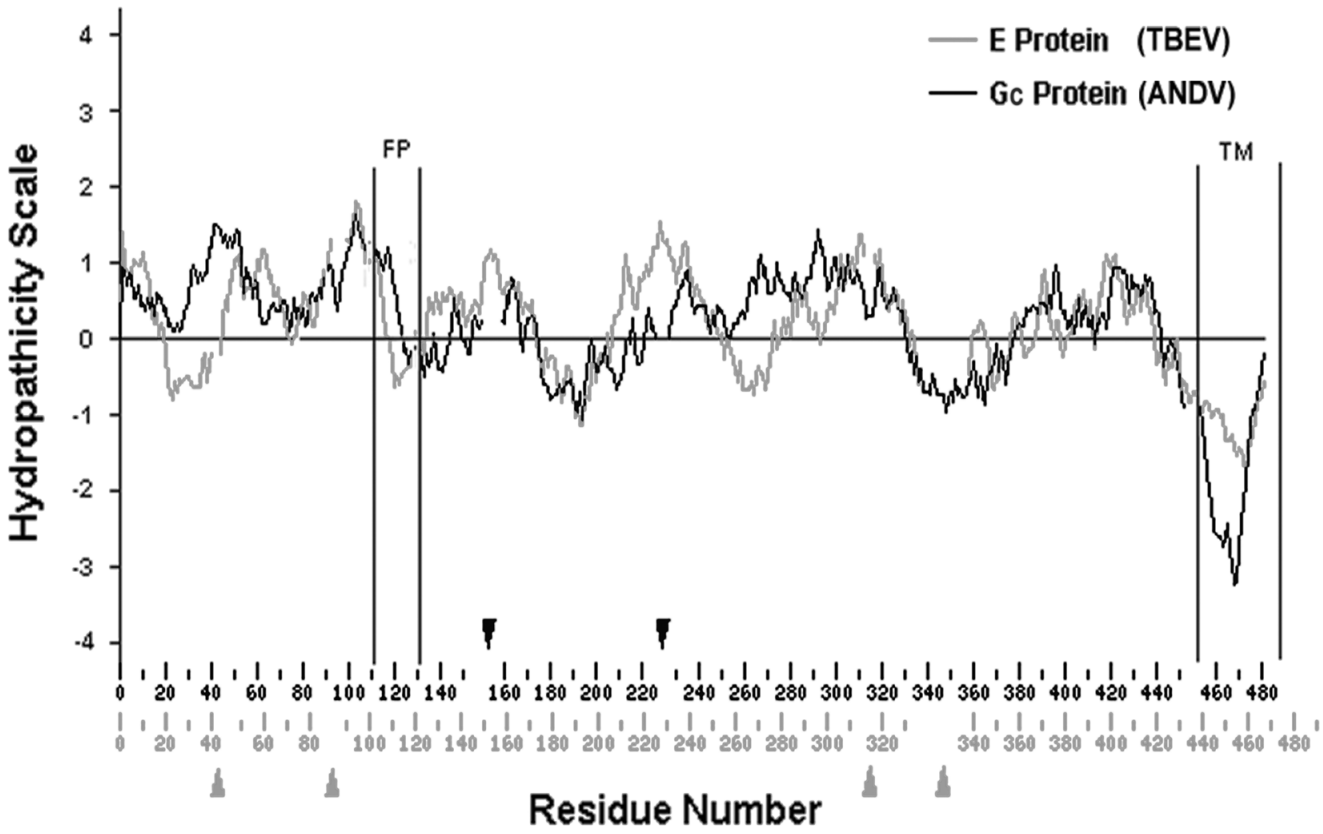

593 **Figure 2. Hydropathic comparison among hantavirus Gc and class II fusion proteins.**

594 Graph indicates the hydropathicity of ANDV Gc and TBEV E proteins along the entire protein

595 length. Vertical bars indicate FP and TM region of the E protein. Arrows indicate gap insertions in

596 the corresponding sequences used to fit the profiles.

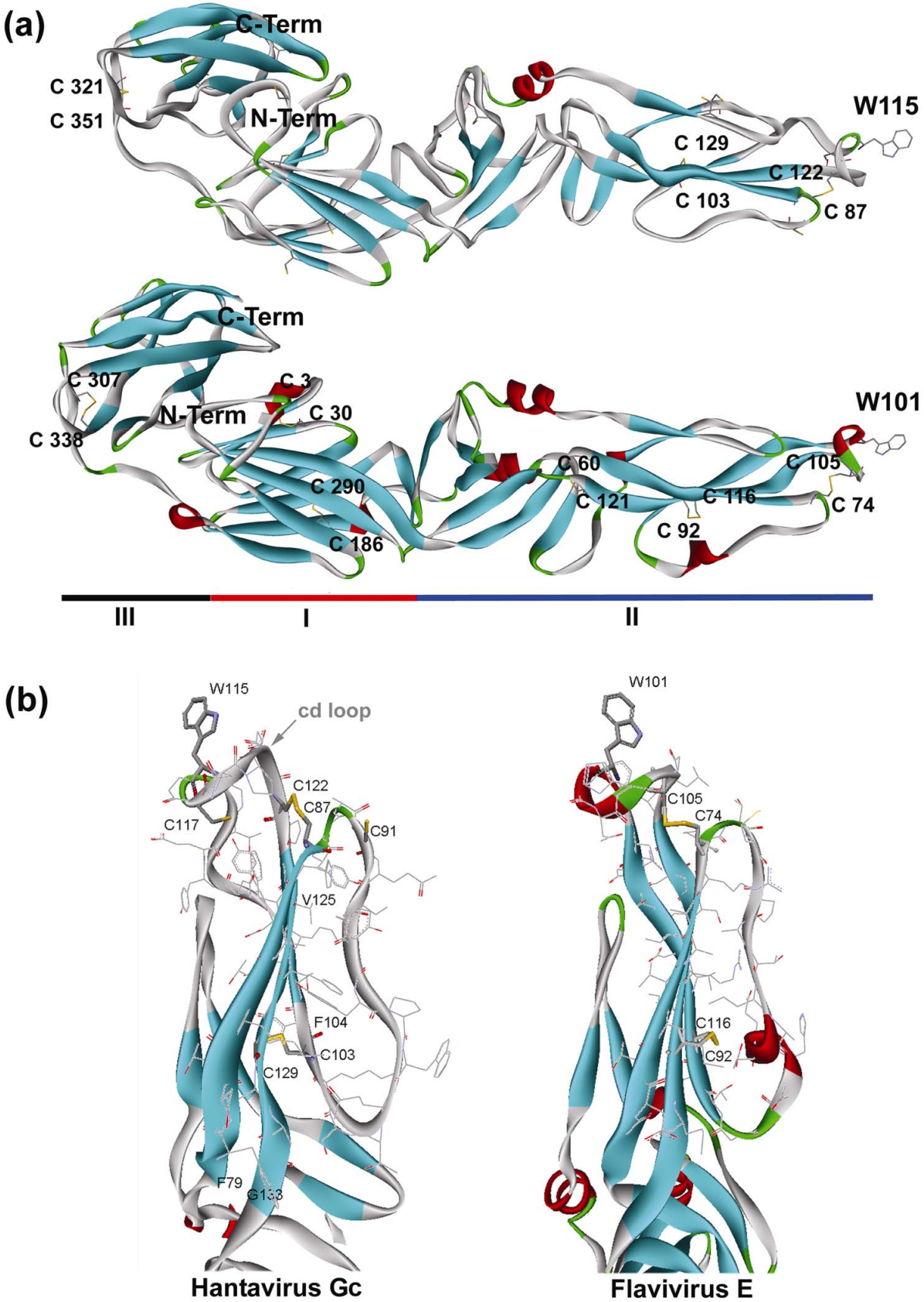

Figure 3. ANDV Gc molecular model and comparison with template structures.

a) Backbone structure comparison of ANDV Gc protein model (top) and TBEV E protein (1SVB) (bottom). Coloured ribbon render indicates the secondary structure using the Kabsch-Sander nomenclature (Kabsch & Sander, 1983). Cys residues involved in disulfide bridges appear yellow labelled and stick represented, Trp at the end of domain II in the cd-loop region is also stick represented. The horizontal bar at the bottom shows the domain organization described for class II fusion proteins.

b) Detailed view of the fusogenic domain of TBEV E and homologous domain in the ANDV Gc model.

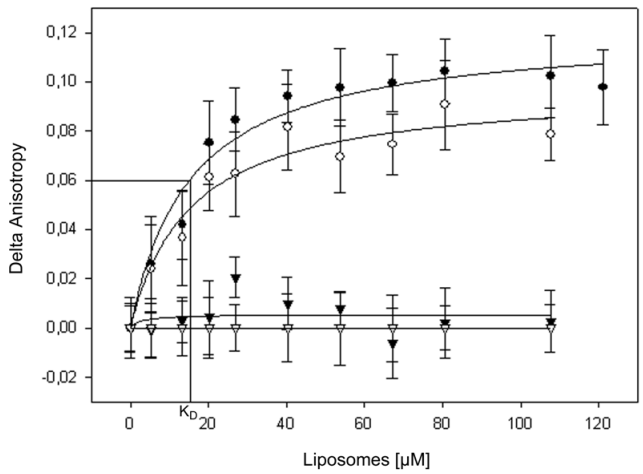

Figure 4. Fusion peptide candidate binding to artificial membranes.

Fluorescence anisotropy gain of peptides as a function of liposome concentration. Peptides [10 µM] were incubated with large unilamellar vesicles (phosphatidylcholine:phosphatidylethanolamine:sphingomyelin:cholesterol 1:1:1:1.5) and anisotropy was measured at different vesicle concentrations. The following samples are indicated: ● Gc-cd1; ○ Gc-cd2; ▼ negative control peptide; ▽ tryptophan.